Statistical bit-error modeling of shallow water acoustic communication links

Mandar Chitre, Konstantinos Pelekanakis, and Matthew Legg

***Abstract*—Underwater network simulation and performance analysis require accurate packet error models. The packet error probability depends on the packet length and the temporal distribution of bit errors. We analyze error traces from the SPACE'08 experiment and show that clustering of errors occurs at several time-scales. We propose a two-part statistical error model consisting of a generalized Pareto fractal renewal parent process that drives Bernoulli daughter processes with generalized extreme value distributed lifetimes. We present an algorithm to simulate communication errors using this error process model and show that the simulated packet loss probability accurately matches experimental observations.**

***Index Terms*—Underwater communications, bit errors, packet errors, generalized Pareto renewal process.**

I. Introduction

Underwater communication performance in terms of data rate and robustness has improved significantly over the past few decades. Underwater acoustic modem technology has therefore matured to a level where underwater networks can be deployed and tested. However, the cost, logistics, and effort involved in deploying experimental underwater networks remains high, and is beyond the reach of many researchers. Even researchers who have access to resources for experimental research in underwater networks prefer to test their networks in simulation prior to experimental testing. Thus, the need for accurate underwater network simulators is key to the future of underwater networking research.

Some underwater networking researchers have customized network simulators (e.g. Omnet++, Opnet, Qualnet, ns-2) while others have chosen to develop their own discrete event simulators. More recently, the idea simulating and experimentally testing underwater protocols with identical implementations (source code) has become popular [1], [2], [3], [4]. In all of the cases, an underwater physical layer performance model is required by the simulator to model the packet loss performance for each link in the network. Although sophisticated physics-based time-varying channel models can be used to determine the errors in each transmitted packet, this approach is computationally infeasible for large-scale simulation. Rather than compute the errors for each packet, some simulators (e.g. WOSS) use acoustic propagation modeling to estimate the packet loss probability [5]. The packet loss probability is then used to simulate packet errors. Although this provides a feasible solution for static networks, the computational load in case of mobile networks is prohibitively large as the acoustic modeling has to be performed every time a node moves. In addition, the computationally feasible physical models may not model all the factors affecting communication performance and therefore may not be able to model the variability in the channel accurately. To reduce complexity further, some researchers use simple range-dependent packet loss probability to model the performance of each link [1]. The computation of the packet loss probability assumes independent bit errors and a constant probability of bit error for a given range. Although useful as a first-order approximation with very low computational complexity, this approach fails to capture the time variability in the channel and the consequent clustering of errors that occurs in underwater channels. Statistical finite state Markov models have been used to model time-variability in packet loss rates [6], [7]. Although hidden Markov models have been shown to model the packet loss of the JANUS modulation scheme during a specific experiment [7], it is not known if these models are generally applicable. Moreover, since the packet error rate (PER) depends on packet size, distinct models are required for different packet sizes.

To partially alleviate the problems described above, we apply statistical modeling to bit errors rather than packet loss. Specifically, we statistically characterize bit error traces from a channel-estimate-based decision feedback equalizer (DFE) by analyzing signals from the SPACE'08 experiment. Using the data collected, we propose a statistical model for the occurrence of errors in a data stream. This model can then be used to compute realistic time-varying packet loss probability for use in analytical network performance modeling and network simulation.

The rest of this paper is organized as follows. In section II, we describe the experiment and data processing which led to the bit error traces that we analyze. In section III, we show that the error traces exhibit clustering at several scales and demonstrate the effect of this on packet loss probability. We show that the long time-scale clustering can be modeled using a fractal renewal process, while shorter time-scale clustering can be approximated by a limited lifetime Bernoulli process. In section IV, we integrate our findings into a statistical model for the error process. We show that this model predicts experimentally observed packet loss probability accurately. Finally in section V, we discuss the implications of this model as well as some of its shortcomings. We also suggest directions for further research in this area.

M. Chitre is with the Electrical & Computer Engineering Department and the ARL, National University of Singapore, Singapore 119227 (e-mail: mandar@arl.nus.edu.sg).

K. Pelekanakis and M. Legg are with the ARL, National University of Singapore, Singapore 119227.

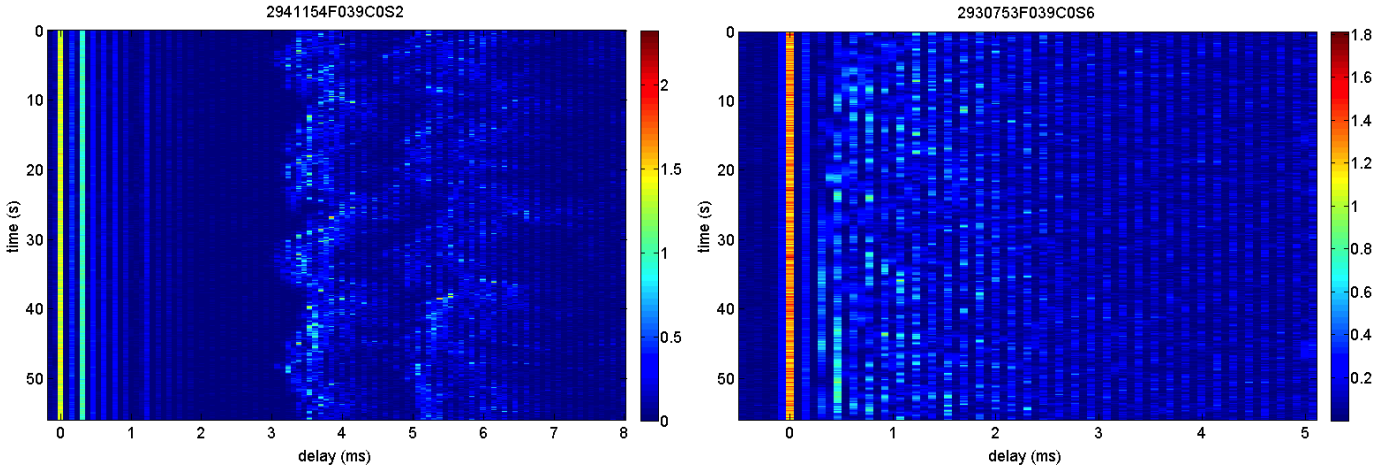

Fig. 1. Representative impulse response from the 80 m (left) and 1 km (right) links. The horizontal axis represents multipath delay and the vertical axis represents absolute time. The colorbar is in a linear scale. The snapshots are generated at the bit rate.

II. Data Collection

The experimental data used for the analysis in this paper were recorded during the SPACE'08 experiment off the coast of Martha's Vineyard, MA, USA in 2008. The transmitter and receiver were static and were located 4 m and 3.25 m, respectively, above the sea floor. The water depth was about 15 m. The transmitted signal was a 6510.4 bps binary phase-shift keying (BPSK) pseudo-noise (PN) sequence that was modulated on to a 12.5 kHz carrier. The source level was 185 dB re 1 μPa @ 1m. Data from two horizontal ranges (80 m and 1000 m) was used in the analysis presented in this paper.

The receiver employed a channel-estimate-based decision feedback equalizer (CEB-DFE), namely, the inter-symbol interference (ISI) was canceled by combining previous channel estimates and symbol decisions before adaptive feedforward (FF) equalization. Channel estimation was performed by employing a novel sparse adaptive algorithm [8], [9]. The FF equalizer was centered around the direct arrival and was adapted to channel variations via the recursive least square (RLS) algorithm. Representative impulse responses for the channels are shown in Fig. 1.

The demodulated data was compared with the transmitted PN-sequence to form error traces. Each error trace was generated from a 1 minute dataset with about 3.6×10^5 bits. The error trace was only collected once the equalizer switched to a decision-directed mode after an initial training period of 500 bits. Three error traces (denoted by F38S2DD, F39S2DD and F40S2DD) were obtained for the 80 m channel, and another three error traces (F38S6DD, F39S6DD and F40S6DD) were obtained for the 1 km channel. In the decision-directed mode we expected some error feedback leading to error propagation in the traces. To guide our understanding of the underlying error generation process with minimal error feedback, we also generated error trace data for the equalizer running in training mode for the entire dataset. These training mode error traces corresponding to F38S2DD, F39S2DD and F40S2DD are denoted by F38S2TR, F39S2TR and F40S2TR respectively.

III. Data Analysis

A. Bernoulli error process model

As a first-order approximation, the error process is often modeled as a Bernoulli process with a constant and independent probability b of bit error. In this model, the number of bit errors in a window of length n bits follows a Binomial distribution with mean nb and variance $nb(1-b)$. The ratio of the variance to the mean of the finite interval count distribution of a point process is known as the *normalized variance* or *Fano factor* [10]. For a Binomial distribution, the Fano factor is $1/(1-b)$ and therefore independent of the window size n. For small b, the Fano factor is expected to be close to 1. The Fano factors for the six decision-directed error traces are shown in Fig. 2. The Fano factors for all error traces are clearly dependent on n. For large n, the Fano factors are much larger than 1 suggesting clustered occurrence of errors.

The error count distribution in a window is directly related to the probability of packet error. A packet of length n is successfully received if there are no bit errors in the packet[1]. For a Bernoulli error process, the probability p of packet error is therefore given by

$$p = 1 - (1-b)^n. \tag{1}$$

By dividing an error trace into non-overlapping packets of n bits each and counting what fraction of the packets are error-free, we can obtain an estimate of the packet error probability p. In Fig. 3, we compare the estimated packet error probability with the prediction from the Bernoulli model for two representative error traces. The Bernoulli model for each of the error traces uses a bit error probability estimate $b = E/N$ where E is the total number of errors and N

[1]If a forward error correction (FEC) code is used, this requirement for no bit errors refers to the output of the decoder.

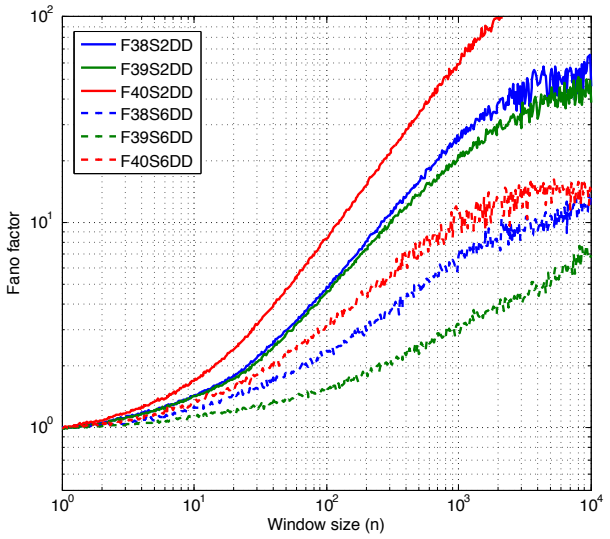

Fig. 2. Fano factor plot of error traces in decision-directed mode.

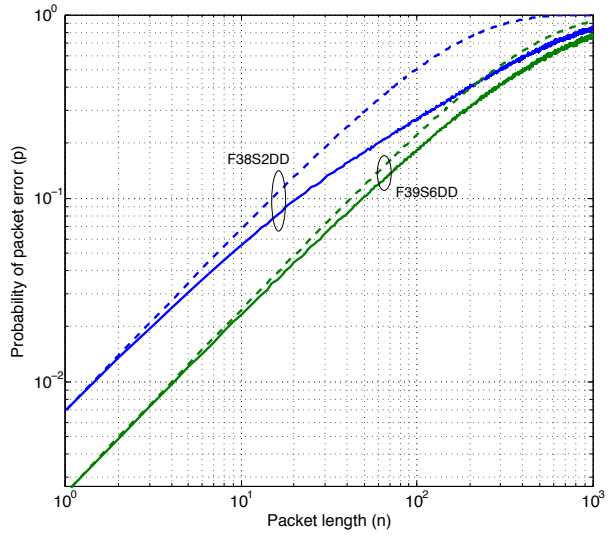

Fig. 3. Probability of packet error for two decision-directed error traces (one each from the 80 m and 1 km channels). The solid line shows the estimated packet error probability from the error trace, while the dashed line shows the corresponding packet error probability predicted by the Bernoulli error model with an estimated bit error probability.

is the total number of bits in that trace. At short packet lengths the model provides a good estimate of packet error probability, but as the packet length increases the predicted probability deviates from the observed probability. It is worth noting that the difference in predicted and measured packet loss probability is loosely related to the deviation of the Fano factor from unity. Due to error clustering observed in terms of increased Fano factor, the Bernoulli model overestimates the packet error probability.

From the above analysis, we see that the Bernoulli process is a poor model for the errors in our datasets. The observed errors are clustered far more tightly than the Bernoulli model predicts. One possibility is that variations of the acoustic

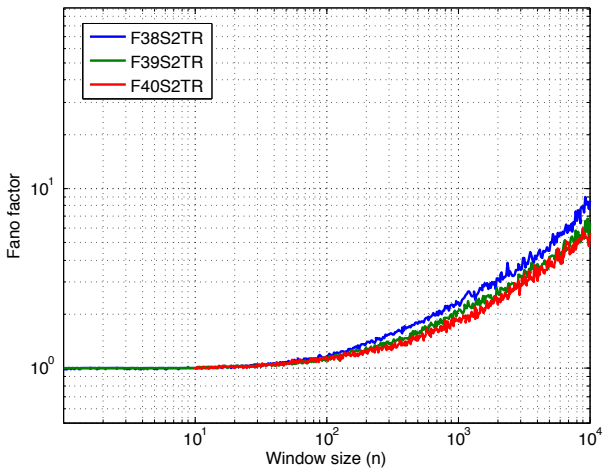

Fig. 4. Fano factor plot of error traces in training mode.

channel over short time-scales (our dataset is only one minute long) may give rise to time-varying error probability. Another possibility is that the decision feedback process in the decision-directed mode may temporarily increase the error probability once an error occurs. To differentiate between these two possibilities, we next study the training mode error traces.

B. Training mode errors

In the decision-directed mode, erroneous decision feedback in the receiver potentially leads to error clusters over short time-scales. To understand how much of the observed deviation from the Bernoulli model are due to this effect, we study the Fano factor plots for the training error traces (see Fig. 4). The Fano factor curves are very different from those in Fig. 2. For small values of n, the Fano factor for the training error traces stays close to 1. Thus a Bernoulli process with a small bit error probability seems to model our training error traces at very short time-scales, suggesting that erroneous decision feedback is primarily responsible for the observed error clustering over these time-scales. The increase in Fano factors at larger n indicates clustering at longer time-scales due to variability in the acoustic channel.

C. Fractal renewal process model

The shape of the Fano factor curves in Fig. 4 is characteristic of Fano factor curves for fractal renewal processes [11], [12]. A *renewal process* is a point process where the interval between adjacent events (errors) is independent and identically distributed (i.i.d.). A *fractal renewal process* is a renewal process where the interval distribution exhibits certain fractal scaling properties. Essentially, a fractal renewal process is self-similar at different time-scales. Inspired by this similarity in Fano factor curve shapes, we next explore whether a fractal renewal process is able to model the longer time-scale error clustering due to channel variability.

As this section focuses on the longer time-scale clustering due to channel variability, we start by filtering the decision-directed error traces to remove short-term clustering due to

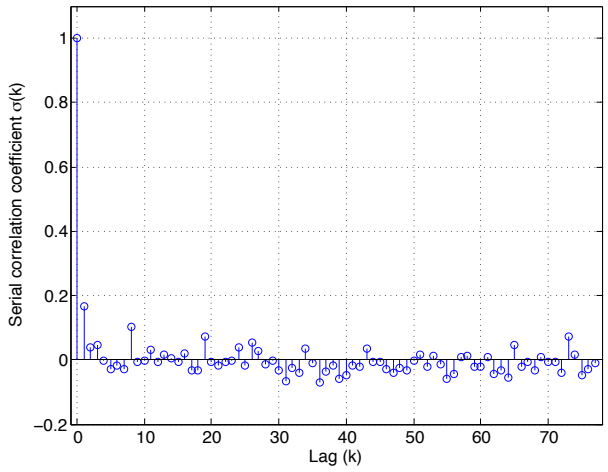

Fig. 5. Interval serial correlation coefficient $\sigma(k)$ for a filtered F38S2DD error trace with T = 50 bits. The serial correlation coefficient plots for other filtered error traces look very similar.

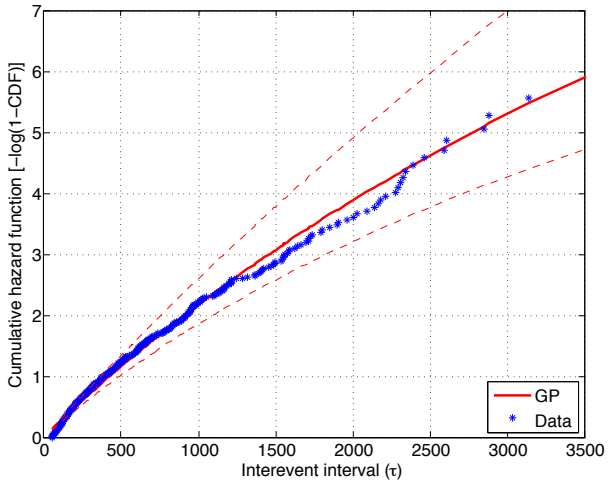

Fig. 6. Interval cumulative hazard function for a filtered F38S2DD error trace with T = 50 bits, along with a GP fit (ξ = 0.12, ψ = 402) to the data. The dashed lines are the 95% confidence interval guides. The cumulative hazard plots for other filtered error traces have similar goodness of fit.

erroneous decision feedback. Let $\{t_i \; \forall \; i \in \mathbb{N}_0\}$ be the set of error locations in the error trace, ordered such that $t_{i-1} < t_i$. Let the interval $\tau_i = t_i - t_{i-1} \; \forall \; i > 0$. The filtered error trace is then given by $\{t_i \; \forall \; \tau_i > T\}$ for some threshold T. The rest of the analysis in this section is presented on the filtered error traces with T = 50 bits.

The *interval serial correlation coefficient* $\sigma(k)$ is a measure of dependence between intervals at lag k in a point process:

$$\sigma(k) = \frac{\mathbb{E}[\tau_i \tau_{i+k}] - \mathbb{E}[\tau_i]^2}{\mathbb{E}\left[\left(\tau_i - \mathbb{E}[\tau_i]\right)^2\right]} \tag{2}$$

where $\mathbb{E}[\cdot]$ is the expectation operator over i. For a renewal process, $\sigma(0) = 1$ and $\sigma(k) = 0 \; \forall \; k \neq 0$. Fig. 5 shows the measured $\sigma(k)$ as a function of k for the filtered error trace of F38S2DD. The values of $\sigma(k)$ for $k > 0$ are small. The filtered process thus shows no dependency between inter-error intervals as would be expected of a renewal process. Similar results are obtained for all six error traces.

The *generalized Pareto* (GP) distribution [13] has tail probability with fractal scaling properties. The cumulative distribution function (CDF) of the GP distribution is given by:

$$F(\tau) = 1 - \left(1 + \xi \frac{\tau}{\psi}\right)^{-1/\xi} \tag{3}$$

where ξ is a shape parameter and ψ is a scale parameter of the distribution. We find that this distribution models the interval probability distribution accurately. Fig. 6 shows the estimated cumulative hazard function[2] of the interval distribution of the F38S2DD error trace along with the a GP fit estimated using the `gpfit` function in MATLAB. Similar results are obtained for all six error traces.

We perform statistical testing of a generalized Pareto renewal (GPR) model using the time transformation tests of Ogata [14]. The time transformation tests make use of the *time-rescaling theorem* [15, Theorem 6]. If the model point process has an identical conditional intensity function[3] to the observed error process then the transformed point process will be consistent with a homogeneous Poisson process with unity rate (Poisson parameter $\lambda = 1$). Ogata uses the term *residual process* to describe the transformed process. Testing on the residual process is therefore a test for a homogeneous Poisson process with unity rate. Berman's test [14] compares modified intervals of the residual process with a uniform distribution on $[0, 1)$. Testing requires parameters for the GP distribution be estimated from the data. To partially alleviate the testing consequences of this estimation, we partition the data into two processes of equal size, estimate parameters from one partition and test on the other partition. Fig. 7 shows the result Berman's test for the residual of the filtered F38S2DD process displayed using the style of a two-sided single sample Kolmogorov-Smirnov test. Shown with the test results are 95% and 99% confidence intervals (two sets of outer dashed lines). The test results are bounded by both of these confidence intervals. In [14] it is observed that while Berman's test is passed, it is quite possible to have clustering in the residual process. For this reason we also show a Fano factor plot of the residual process with 99% confidence intervals in Fig. 8. The confidence intervals assume a χ^2 distribution of uncertainty in the Fano factor and is suitable for testing for a homogeneous Poisson process [16]. The Fano factor plots show that there is no significant clustering in the residual process. Ogata also suggests testing using the empirical log-survivor function and Pouzat [17] suggests a Wiener process test. These additional tests were performed and the results were consistent with a GPR process.

From the analysis presented above, we see that a GPR

[2]For a random variable with CDF $F(\tau)$, the cumulative hazard function $H(\tau) = -\log\left(1 - F(\tau)\right)$.

[3]The intensity function of a point process at time t is defined as $\lim_{\Delta t \to 0} \mathbb{P}(\text{one event occurs in time } [t, t + \Delta t])/\Delta t$.

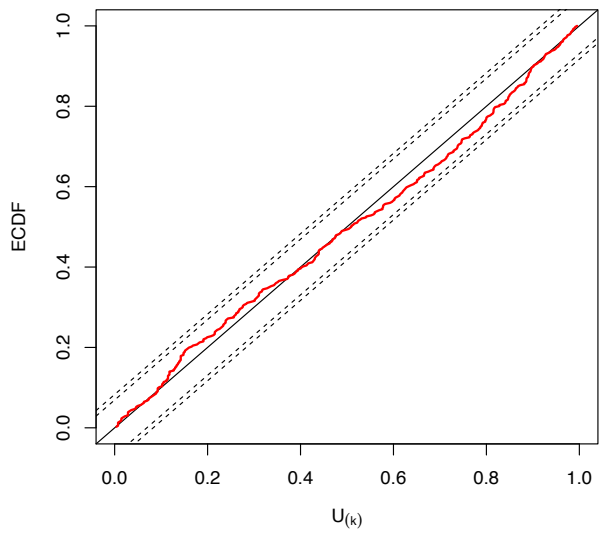

Fig. 7. Berman's test applied to the residual process after time transformation of the filtered F38S2DD error trace with T = 50 bits. The distribution function plotted as a function of modified intervals U_k is expected to lie on a straight line. Shown here are the empirical CDF of the intervals from the residual process (solid red line) and the 95% and 99% confidence intervals from the Kolmogorov-Smirnov test (dashed black lines).

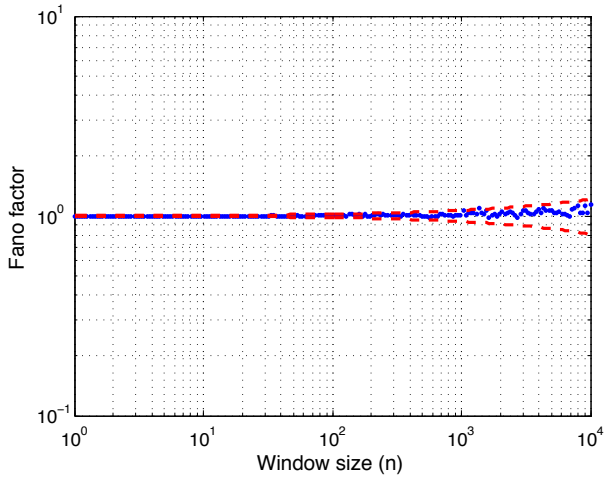

Fig. 8. Fano factor plot for the residual of the filtered F38S2DD error trace with T = 50 bits. This plot shows that there is no significant residual clustering in the process after time transformation using a GP model. 99% confidence intervals assuming a χ^2 distribution are shown (dashed red lines).

process accurately models the long time-scale errors in the datasets we analyzed.

D. Short-term clustering due to decision feedback

Modeling of the short-term clustering due to the feedback of erroneous decisions is harder. We assume that the long time-scale error process is a *parent process* that drives a short time-scale *daughter process*. Every time the parent process generates an error, a daughter process is instantiated. This process generates a cluster of errors that lasts for a finite but random length of time. The daughter process represents the

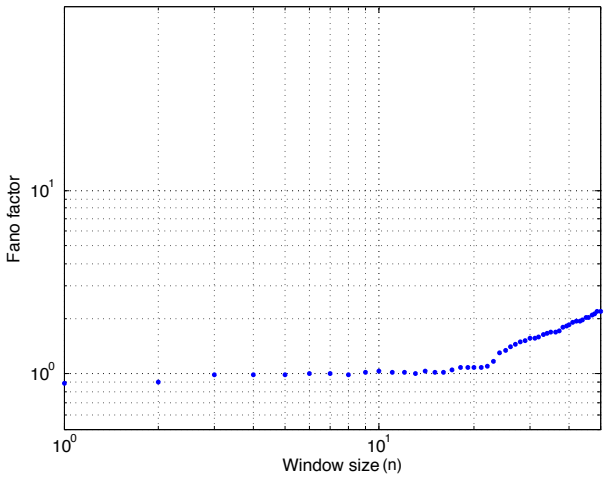

Fig. 9. An averaged Fano factor plot for all daughter processes derived from F38S2DD error trace with T = 50 bits. The plot is consistent with a Bernoulli process at short time-scales. Similar results are obtained for other error traces.

effect of the erroneous feedback in the receiver system. Although the general parent-daughter process structure is likely to be generally applicable, the exact model for the daughter process will depend strongly on the receiver structure.

It is impossible to completely separate the errors from the parent and daughter process in an error trace. However we obtain estimates of the daughter process corresponding to each parent process event using the following technique: We mark the errors from the parent process using the filtering technique outlined in the previous section. All remaining errors in the error trace are then assigned to a daughter process corresponding to the preceding parent process error. The length of each daughter process is the number of bits between the corresponding parent process error and the last error from the daughter process.

An averaged Fano factor plot for all daughter processes derived from the F38S2DD error trace using the technique in the previous paragraph is shown in Fig. 9. At short window sizes the Fano factor is close to unity, suggesting a Bernoulli process model at short time-scales. As the window size increases beyond 20, the Fano factor systematically grows; this may be attributed to contamination from the parent process and from the truncation of the daughter process due to the filtering. Recall that the filtering was performed with T = 50 bits and therefore one would expect significant deviation as the window size approaches 50. Similar results are obtained for all six error traces.

The probability distribution of the length of the daughter process was empirically derived from the F38S2DD error trace. By testing several common probability distributions, we found that the *generalized extreme value* (GEV) distribution [18] offered the best fit. The CDF of the GEV distribution is given by:

$$F(z) = \exp\left[-\left(1+\xi\frac{z-\mu}{\psi}\right)^{-1/\xi}\right] \qquad (4)$$

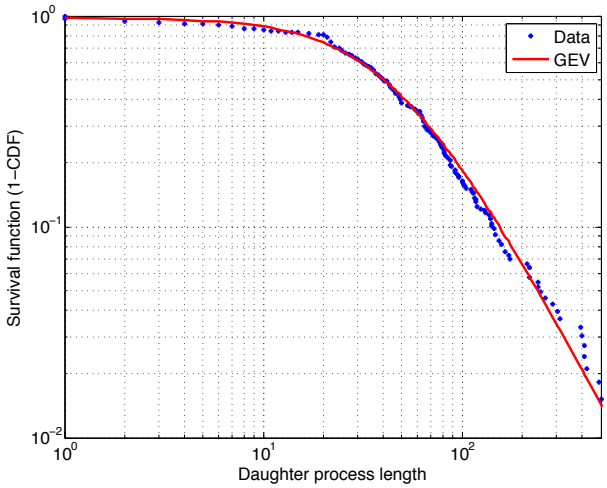

Fig. 10. Daughter length survival function (1-CDF) for a F38S2DD error trace with T = 50 bits, along with a GEV fit (ξ = 0.54, ψ = 29, μ = 28) to the data. Similar goodness of fit are obtained for other error traces.

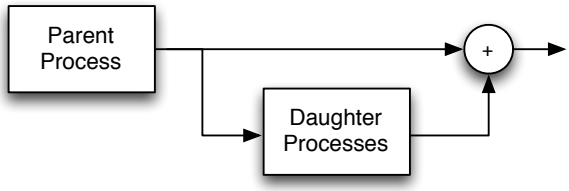

Fig. 11. Block diagram of the overall error generation process model.

where ξ is a shape parameter, ψ is a scale parameter and μ is a location parameter. The survival function[4] estimated from the data and the best fit GEV computed using the `gevfit` function in MATLAB are shown in Fig. 10. Similar results are obtained for other error traces.

IV. Error Process Model

Based on the findings discussed in section III, we propose a statistical model for bit errors in an underwater communication stream. The model consists of a parent process and a number of daughter processes as shown in Fig. 11. The parent process is a GPR process that generates errors at intervals drawn from a GP distribution. Each error in the parent process results in a daughter process with a finite lifetime drawn from a GEV distribution. During the life of the daughter process, she generates additional errors in accordance with a Bernoulli process.

The model is characterized by 6 parameters – ξ_1 and ψ_1 for the GP distribution, ξ_2, ψ_2 and μ_2 for the GEV distribution, and the error probability b for the Bernoulli distribution. A simple algorithm to generate errors according to this error process model is given in Algorithm 1.

To validate our model, we simulate error traces in a communication stream with 10^6 bits using Algorithm 1. By dividing each bit steam into non-overlapping packets of length n, we compute the packet error probability p for the simulated error trace as a function of n. For the two datasets previously analyzed in Fig. 3, we compare the packet error probability curves from the experimental error traces and two simulation runs. The simulation for each of the dataset uses model parameters estimated from the dataset. As seen in Fig. 12, the simulated packet error curves closely matched the measured curves. The proposed error process model generates errors with appropriate clustering to yield the observed packet error probability for any packet length.

[4]For a random variable with CDF $F(\tau)$, the survival function $S(\tau) = 1 - F(\tau)$.

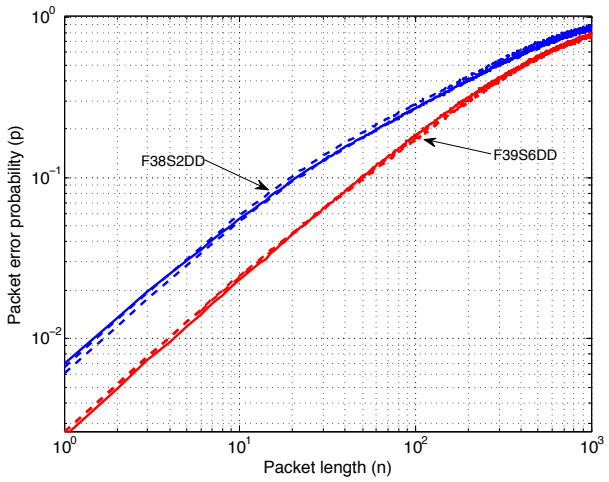

Fig. 12. Probability of packet error for two decision-directed error traces (one each from the 80 m and 1 km channels). The solid line shows the estimated packet error probability from the error trace, while the dashed lines show corresponding packet error probabilities from two simulation runs of the proposed error model.

Algorithm 1 Algorithm to generate errors according to the proposed error process model.

Require: Model parameters: ξ_1, ψ_1, ξ_2, ψ_2, μ_2, b
Require: N is the number of events to simulate
Ensure: π is a set of error locations

$t \leftarrow 0$
$\pi = \emptyset$
for $i = 1 \rightarrow N$ **do**
  $\tau \leftarrow$ random number drawn from GP(ξ_1, ψ_1)
  $t \leftarrow t + \tau$
  $\pi \leftarrow \pi \cup \{\lfloor t \rceil\}$
  $\lambda \leftarrow$ random number drawn from GEV(ξ_2, ψ_2, μ_2)
  for $j = 1 \rightarrow \lfloor \lambda \rceil$ **do**
    $v \leftarrow$ uniform random number between 0 and 1
    if $v < b$ **then**
      $\pi \leftarrow \pi \cup \{t + j\}$
    end if
  end for
end for

V. Discussion and Conclusions

We analyzed six different error traces derived from minute-long recordings at ranges of 80 m and 1 km during the SPACE'08 experiment. We showed that packet error probability computations using an average BER derived from the error traces and a Bernoulli error process assumption were inconsistent with experimentally measured PER. The mismatch was found to be primarily due to clustering of errors that occurs at several time-scales. Based on the analysis of the clustering, we proposed a two-part statistical error model. The model consists of a GPR parent process that drives Bernoulli daughter processes with GEV distributed lifetimes. We presented an algorithm to simulate communication errors using this error process model and showed that the simulated PER accurately matches the experimentally observed PER. Hence we conclude that the error process model we proposed captures the important aspects of the error generation process.

The GPR process is a fairly general fractal renewal point process. Although our error traces were obtained from a coherent single carrier communication system using a channel estimate based DFE, we believe that this GPR process model is general enough for use with other receiver structures as well. This belief is further strengthened by the noting that renewal processes with Pareto distributed intervals have previously been used to model other channels and receivers [19], [20].

The Bernoulli daughter process with GEV distributed lifetimes is somewhat more empirical and perhaps specific to the receiver structure or the experimental setup we used. Analysis of error traces from other underwater communication experiments is required to help determine how generally applicable this process model is. However, since the daughter process operates over very short time-scales, the errors generated by this process are often contained within a single packet for typical packet lengths of interest. Since the driving parent process already corrupts the packet that contains the daughter process errors, the exact structure of the daughter process error cluster becomes unimportant in analysis of packet error performance. Packet loss computations can therefore be expected to be relatively robust to model mismatch in the daughter process.

Acknowledgement

The authors would like to thank Dr. James C. Preisig for conducting the SPACE'08 experiment that provided valuable data for this work.

References

[1] S. Shahabudeen, M. A. Chitre, M. Motani, and Y. S. Low, "Unified Simulation and Implementation Software Framework for Underwater MAC Protocol Development," in *IEEE/MTS Oceans'09 Conference, Biloxi, US*, October 2009.

[2] C. Petrioli, R. Petroccia, J. Shusta, and L. Freitag, "From underwater simulation to at-sea testing using the ns-2 network simulator," in *Proceedings of IEEE OCEANS 2011*. Santander, Spain: IEEE Computer Society, June, 6–9 2011.

[3] R. Masiero, S. Azad, F. Favaro, M. Petrani, G. Toso, F. Guerra, P. Casari, and M. Zorzi, "DESERT Underwater: an NS–Miracle-based framework to DEsign, Simulate, Emulate and Realize Test-beds for Underwater network protocols," in *Proceedings of IEEE OCEANS'12 Yeosu*, 2012.

[4] M. Chitre, "The UNET-2 modem – an extensible tool for underwater networking research," in *Proceedings of IEEE OCEANS'12 Yeosu*, 2012.

[5] F. Guerra, P. Casari, and M. Zorzi, "World ocean simulation system (woss): a simulation tool for underwater networks with realistic propagation modeling," in *Proceedings of the Fourth ACM International Workshop on UnderWater Networks*, ser. WUWNet '09. New York, NY, USA: ACM, 2009, pp. 4:1–4:8.

[6] F. Pignieri, F. De Rango, F. Veltri, and S. Marano, "Markovian approach to model underwater acoustic channel: Techniques comparison," in *Military Communications Conference, 2008. MILCOM 2008. IEEE*, nov. 2008, pp. 1 –7.

[7] B. Tomasi, P. Casari, L. Finesso, G. Zappa, K. McCoy, and M. Zorzi, "On modeling JANUS packet errors over a shallow water acoustic channel using markov and hidden markov models," in *MILITARY COMMUNICATIONS CONFERENCE, 2010 - MILCOM 2010*, 31 2010-nov. 3 2010, pp. 2406 –2411.

[8] K. Pelekanakis and M. Chitre, "Natural gradient-based adaptive algorithms for sparse underwater acoustic channel identification," in *Underwater Acoustic Measurements: Technologies and Results, 4th International Conference and Exhibition, Kos Island, Greece*, June 2011, pp. 1403–1410.

[9] ——, "New sparse adaptive algorithms based on the natural gradient and the L0 norm," *Oceanic Engineering, IEEE Journal of*, 2012 (submitted).

[10] U. Fano, "Ionization yield of radiations. ii. the fluctuations of the number of ions," *Physical Review*, vol. 72, no. 1, p. 26, 1947.

[11] S. Lowen and M. Teich, "Estimation and simulation of fractal stochastic point processes," *Fractals*, vol. 3, no. 1, pp. 183–210, 1995.

[12] ——, *Fractal-based point processes*. Wiley-Blackwell, 2005, vol. 366.

[13] B. Arnold, "Pareto and generalized pareto distributions," *Modeling Income Distributions and Lorenz Curves*, pp. 119–145, 2008.

[14] Y. Ogata, "Statistical models for earthquake occurrences and residual analysis for point processes," *Journal of the American Statistical Association*, vol. 83, no. 401, pp. 9–27, March 1988.

[15] F. Papangelou, "Integrability of expected increments of point processes and a related random change of scale," *Transactions of the American Mathematical Society*, vol. 165, pp. 483–506, March 1972.

[16] U. Eden and M. Kramer, "Drawing inferences from fano factor calculations," *Journal of neuroscience methods*, vol. 190, no. 1, pp. 149–152, 2010.

[17] C. Pouzat and A. Chaffiol, "On Goodness of Fit Tests For Models of Neuronal Spike Trains Considered as Counting Processes," *ArXiv e-prints*, September 2009.

[18] S. Coles, *An introduction to statistical modeling of extreme values*. Springer Verlag, 2001.

[19] J. Berger and B. Mandelbrot, "A new model for error clustering in telephone circuits," *IBM Journal of Research and Development*, vol. 7, no. 3, pp. 224–236, 1963.

[20] B. Mandelbrot, "Self-similar error clusters in communication systems and the concept of conditional stationarity," *Communication Technology, IEEE Transactions on*, vol. 13, no. 1, pp. 71–90, 1965.